

Article

# Rectum Dose Constraints for Carbon Ion Therapy: Relative Biological Effectiveness Model Dependence in Relation to Clinical Outcomes

Kyungdon Choi <sup>1,2,†</sup>, Silvia Molinelli <sup>1,†</sup>, Stefania Russo <sup>1</sup>, Alfredo Mirandola <sup>1</sup>, Maria Rosaria Fiore <sup>1</sup>, Barbara Vischioni <sup>1</sup>, Piero Fossati <sup>3</sup>, Rachele Petrucci <sup>1</sup>, Irene Turturici <sup>4</sup>, Jon Espen Dale <sup>5</sup> , Francesca Valvo <sup>1</sup>, Mario Ciocca <sup>1</sup> and Andrea Mairani <sup>1,6,\*</sup>

<sup>1</sup> Clinical Department, Centro Nazionale di Adroterapia Oncologica, 27100 Pavia, Italy; kyungdon.choi@cnao.it (K.C.); silvia.molinelli@cnao.it (S.M.); Stefania.Russo@cnao.it (S.R.); Alfredo.Mirandola@cnao.it (A.M.); MariaRosaria.Fiore@cnao.it (M.R.F.); Barbara.Vischioni@cnao.it (B.V.); Rachele.Petrucci@cnao.it (R.P.); Francesca.Valvo@cnao.it (F.V.); mario.ciocca@cnao.it (M.C.)

<sup>2</sup> Department of Physics, University of Pavia, 27100 Pavia, Italy

<sup>3</sup> Medical Department, MedAustron Ion Therapy Center, 2700 Wiener Neustadt, Austria; Piero.Fossati@medaustron.at

<sup>4</sup> Department of Diagnostic Imaging, Molecular Imaging, Interventional Radiology and Radiotherapy, University of Roma Policlinico TorVergata, 00133 Roma, Italy; ireneturturici@alice.it

<sup>5</sup> Department of Oncology and Medical Physics, Haukeland University Hospital, 1400 Bergen, Norway; jon.espen.dale@helse-bergen.no

<sup>6</sup> BioPT Group, Heidelberg Ion-Beam Therapy Center, 69120 Heidelberg, Germany

\* Correspondence: andrea.mairani@med.uni-heidelberg.de; Tel.: +49-0-6221-56-37535

† These authors contributed equally to this work.

Received: 7 November 2019; Accepted: 9 December 2019; Published: 21 December 2019



**Abstract:** The clinical application of different relative biological effectiveness (RBE) models for carbon ion RBE-weighted dose calculation hinders a global consensus in defining normal tissue constraints. This work aims to update the local effect model (LEM)-based constraints for the rectum using microdosimetric kinetic model (mMKM)-defined values, relying on RBE translation and the analysis of long-term clinical outcomes. LEM-optimized plans of treated patients, having suffered from prostate adenocarcinoma ( $n = 22$ ) and sacral chordoma ( $n = 41$ ), were recalculated with the mMKM using an in-house developed tool. The relation between rectum dose-volume points in the two RBE systems ( $D_{LEM|V}$  and  $D_{MKM|V}$ ) was fitted to translate new LEM-based constraints. Normal tissue complication probability (NTCP) values, predicting late rectal toxicity, were obtained by applying published parameters. No late rectal toxicity events were reported within the patient cohort. The rectal toxicity outcome was confirmed using dosimetric analysis:  $D_{MKM|V}$  lay largely below original constraints; the translated  $D_{LEM|V}$  values were 4.5%, 8.3%, 18.5%, and 35.4% higher than the nominal  $D_{MKM|V}$  of the rectum volume,  $v = 1\%$ , 5%, 10% and 20%. The average NTCP value ranged from 5% for the prostate adenocarcinoma, to 0% for the sacral chordoma group. The redefined constraints, to be confirmed prospectively with clinical data, are  $D_{LEM|5cc} \leq 61$  Gy(RBE) and  $D_{LEM|1cc} \leq 66$  Gy(RBE).

**Keywords:** carbon ion therapy; RBE modeling; rectum constraints; FROG

## 1. Introduction

The physical and radiobiological characteristics of carbon ion beams, i.e., finite range, inverse depth dose profile, sharp lateral penumbra and increased relative biological effectiveness (RBE) at the end of range, make them suitable and potentially advantageous for the treatment of tumors that

are radio-resistant to conventional radiotherapy and/or in close proximity to critical organs at risk (OARs) [1]. Comparing clinical results obtained with carbon ion radiotherapy (CIRT) at different institutions is, however, not always straightforward—as the reported nominal RBE-weighted doses depend critically on the different RBE models used [2–4].

The Italian National Hadrontherapy Center (CNAO, Pavia, Italy) employs fractionation schedules—derived from clinical experience acquired at the National Institute of Radiological Science (NIRS, Chiba, Japan)—for prostate adenocarcinoma (AdC) and sacral chordoma treatments, while changing the prescription dose to account for the use of different models for plan optimization [3,5]. Particularly, the local effect model (LEM—version I) is employed by European centers [6,7], while Japanese centers use either the semi-phenomenological mixed-beam model [8], or the modified microdosimetric kinetic model (mMKM) [9]. These latter two models have been clinically validated at the NIRS for their consistency and both will be referred to here as mMKM [10].

For the treatment of tumors in the pelvis, radiation-induced rectal damage is a major issue impacting quality of life during and after treatment [11,12]. In conventional radiation therapy, several studies concerning rectum tolerance doses and normal tissue complication probability (NTCP) parameters are available [11,13]; by contrast, CIRT is a fairly novel modality and long-term rectal toxicity data are still under investigation. Despite well-known differences in the two RBE systems outside the target volume, CNAO is following a conservative approach, by prudentially adopting rectum constraints from the experience acquired through NIRS [14,15]. The late rectal toxicity of prostate AdC patients treated at NIRS was recently reported and fitted to the Lyman–Kutcher–Burman (LKB) NTCP model [16]. Additionally, a new study showed that the dose to 2 cc of the rectum volume ( $D_{2cc}$ ) could represent a good predictor of CIRT rectal damage [17].

A fast-forward dose calculation system (FRoG), running on graphics processing units, capable of calculating both LEM and mMKM RBE-weighted doses ( $D_{LEM}$  and  $D_{MKM}$ ) for the same treatment plan, was developed in a collaboration between CNAO and the Heidelberg Ion Therapy Center (HIT, Heidelberg, Germany) [18,19]. In this work, FRoG was used to compute and analyze differences between LEM and mMKM RBE-weighted dose distribution ( $D_{RBE}$ ) to the rectum for prostate AdC and sacral chordoma patients previously treated at CNAO. In parallel, we analyzed clinical outcomes from CNAO in relation to the NIRS rectum toxicity, and applied the NIRS NTCP model [16] to evaluate the expected probability of late rectal damage based on a patient cohort with a longer follow-up period. The main aim was to establish and propose updated LEM-based planning constraints for safe clinical application, correcting the over-conservative approach adopted since the beginning of clinical activity at CNAO.

## 2. Results

Two representative cases, one of prostate AdC and one of sacral chordoma, are shown in Figure 1. Together with the axial view of  $D_{RBE}$  distributions, we also plotted the corresponding clinical target volume (CTV) and rectum dose volume histograms (DVHs), to highlight differences between the two RBE systems. In our clinical practice, dose deviations between LEM and mMKM in the CTV have been partially accounted for [3,5]; while no correction was applied until recently for dose over-estimation in OARs [15].

The best model fitting the relation between LEM and mMKM  $D_v$  was a quadratic regression:

$$D_{MKM|v} = a \times (D_{LEM|v})^2 + b \times D_{LEM|v} + c, \quad (1)$$

Based on the applied model, the translation of the original NIRS  $D_{MKM|v}$  to new  $D_{LEM|v}$  values was made possible: 42.9 Gy(RBE) (confidence interval (CI) 95%: 38.9–46.8), 57.7 Gy(RBE) (54.7–61.0), 68.2 Gy(RBE) (65.1–70.8) and 72.0 Gy(RBE) (69.3–74.8) for  $v$ —20%, 10%, 5% and 1%, respectively. In Figure 2, patient-specific  $D_{MKM|v}$  values are plotted as a function of  $D_{LEM|v}$  for  $v$ —20%, 10%, 5% and 1% of the rectum volume, together with the best fit and corresponding 95% CI.

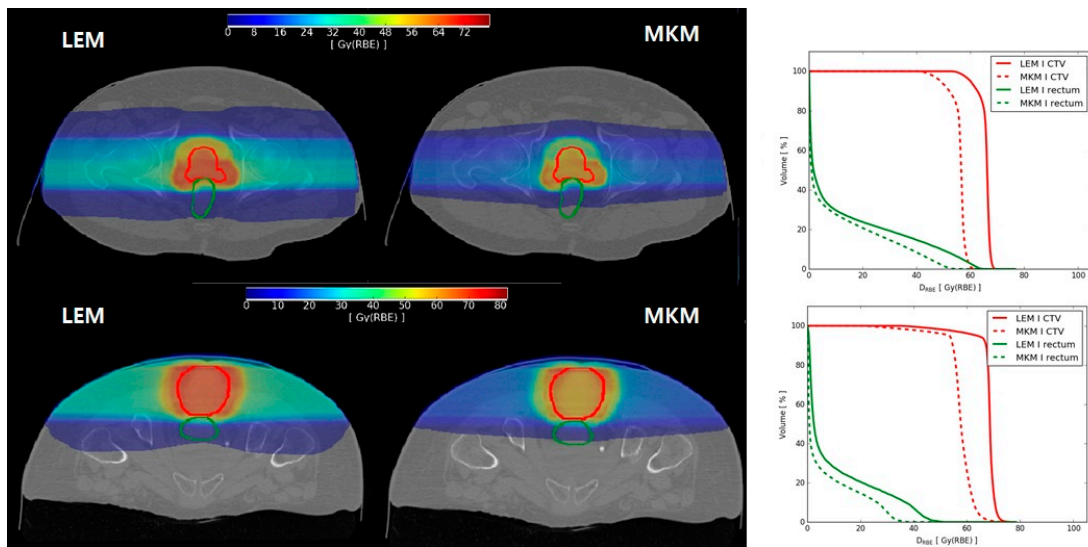


**Figure 1.** Left side: axial view of (upper panel) prostate and (lower panel) sacral chordoma patients local effect model (LEM) and microdosimetric kinetic model (mMKM) RBE-weighted dose distributions with clinical target volume (CTV—red line) and rectum (green line) contours. Right side: corresponding dose volume histograms (DVHs) for LEM RBE-weighted dose ( $D_{LEM}$ ) (solid line) and mMKM RBE-weighted doses ( $D_{MKM}$ ) (dotted line).

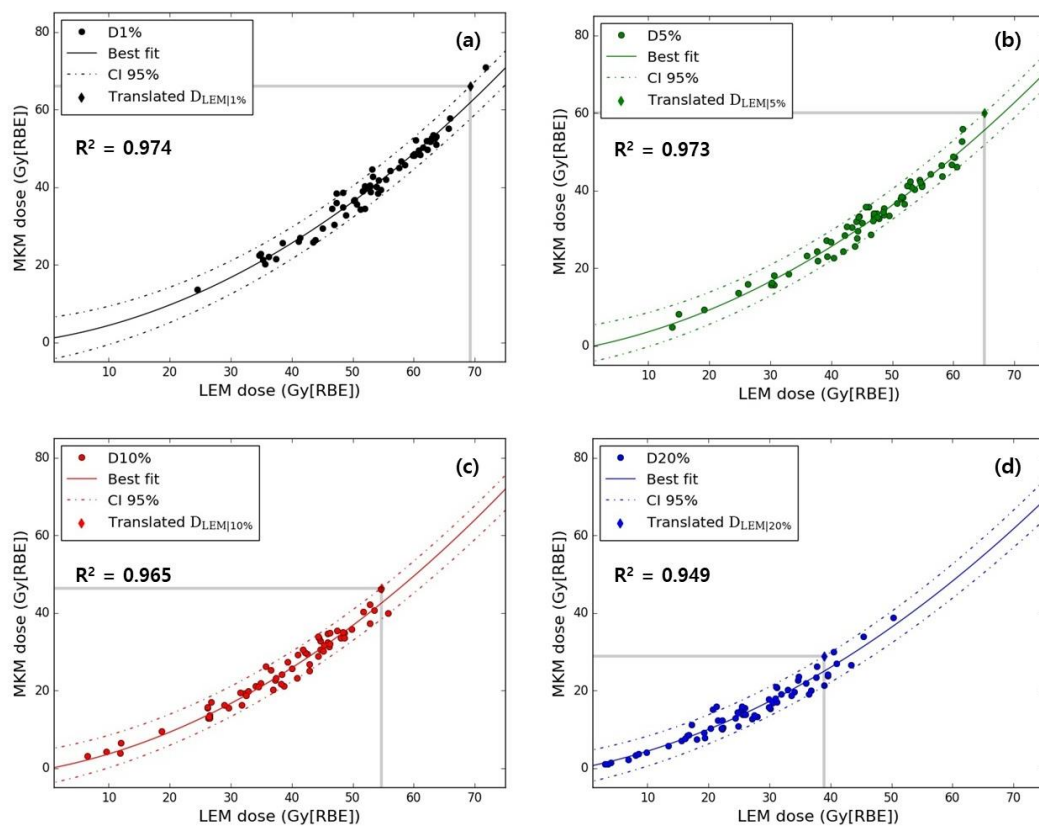


**Figure 2.** Rectum  $D_{MKM}$  as a function of  $D_{LEM}$  for (a)  $D_{1\%}$ , (b)  $D_{5\%}$  (c)  $D_{10\%}$  and (d)  $D_{20\%}$  are presented with the corresponding fitting functions (solid lines represent the best fits and dashed lines represent the 95% confidence interval (CI)). Coefficients of determination ( $R^2$ ) for each parameter are given as well. In each plot, grey lines indicate the original  $D_{MKM|V}$  constraint and corresponding  $D_{LEM|V}$  translation (diamond).

Lower bound CI values will be considered as newly translated  $D_{LEM|V}$  values. Using the lower bound CI, we aimed to take into account the sources of uncertainty involved in the described analysis.

Averaged  $D_{LEM}$  and  $D_{MKM}$  rectum DVHs over the selected patient cohort are shown in Figure 3. The DVH bands represent  $\pm 1$  standard deviation.

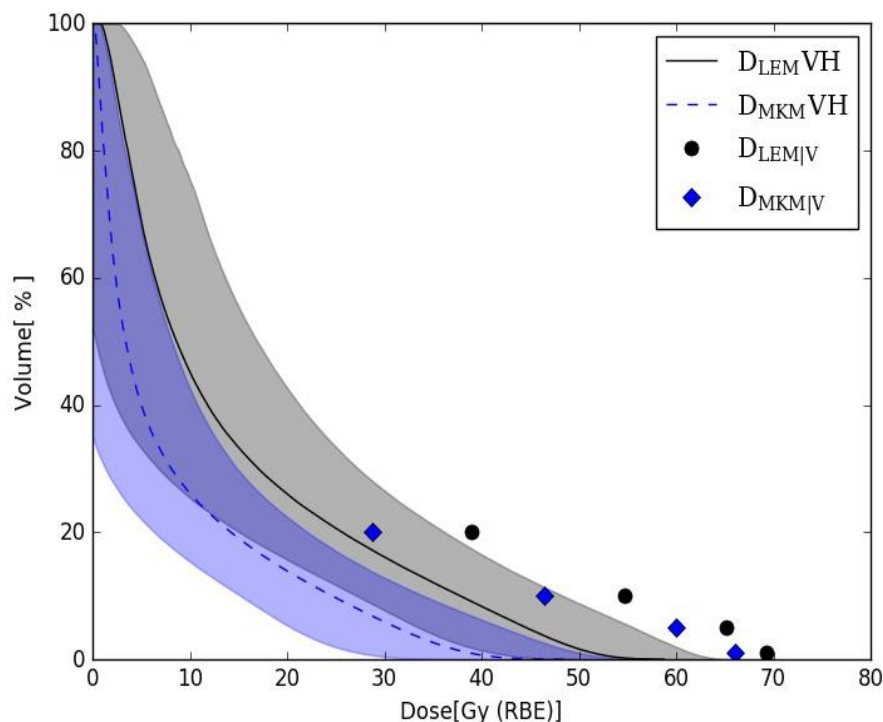


**Figure 3.** Average  $D_{LEM}$  (black solid line—grey band) and  $D_{MKM}$  (blue dotted line—blue band) rectum DVHs with  $D_{MKM|V}$  (blue diamonds) and translated  $D_{LEM|V}$  (black dots) values. DVH bands represent  $\pm 1$  standard deviation.

The prostate AdC and sacral chordoma delivered treatment plans were optimized using LEM-based, RBE-weighted doses while applying  $D_{MKM|V}$  constraints. As shown in Figure 3, the average  $D_{LEM}$  rectum DVH lies under  $D_{MKM|V}$  constraints; with a portion of patient specific DVHs exceeding nominal values.

More specifically,  $D_{LEM}$  VHs exceed the  $D_{MKM|20\%}$  constraint of 28.8 Gy(RBE) in 42.9% of the cases (20 of the sacral chordoma and 7 prostate AdC patients); the  $D_{MKM|10\%}$  of 46.4 Gy(RBE) was exceeded in 1.6% of the patients (one prostate AdC case); the  $D_{MKM|5\%}$  constraint of 60 Gy(RBE) was exceeded in 3.2% of the cases (two prostate AdC case); no case exceeded the  $D_{MKM|1\%}$ , of 66 Gy(RBE).

In clinical practice, the constraints for OARs are compromised when priority is given to target coverage. No increase in complication rate was determined by the high percentage of  $D_{LEM}$  VHs exceeding  $D_{MKM|20\%}$ . On the other side, only 3.2% (two prostate AdC cases) of  $D_{MKM}$  VHs exceeded  $D_{MKM|20\%}$ . When relating to the translated  $D_{LEM|V}$  constraints, the percentage of non-compliant  $D_{LEM}$  VHs drastically decreased to 3.2% for  $D_{LEM|20\%}$  (consisting in the same two prostate AdC patients resulting from the mMKM analysis), and 0% for the other volume points, in perfect agreement with the mMKM scenario.

A total of five patient plans (2 prostate cases, 2  $L_{SAC}$  cases and 1  $H_{SAC}$  case) were re-optimized with translated  $D_{LEM|V}$  values and re-calculated with FRoG to analyze the rectum  $D_{MKM}$  VHs. Table 1 presents both  $D_{LEM|V}$  and  $D_{MKM|V}$  ( $v$ : 20%, 10%, 5%, 1% of the rectum volume) values for the newly optimized plans, to be compared with the reference constraints, expressed in the corresponding RBE language. From the recalculation of mMKM RBE-weighted dose distributions for the five plans, we demonstrated that nominal  $D_{MKM|V}$  constraints were still respected, confirming the predictive

power of the adopted regression model.  $D_{20\%}$  and  $D_{10\%}$  were not applied during optimization of the sacral chordoma plans and, therefore, values exceeded the constraints in both LEM- and mMKM-based scenarios.

**Table 1.** Rectum  $D_{LEM|v}$  and  $D_{MKM|v}$  ( $v$ : 20%, 10%, 5%, 1% of the rectum volume) for five patients’ treatment plans (two prostate AdC cases, two Sacral chordoma cases from the  $L_{SAC}$  group, and one case from the  $H_{SAC}$  group), optimized with translated  $D_{LEM|v}$  constraints. The old  $D_{MKM|v}$  and translated  $D_{LEM|v}$  constraints are reported in brackets in the corresponding column heading. The rectum volume of each patient is also presented.  $D_{20\%}$  and  $D_{10\%}$  were not applied for sacral chordoma plan optimization.

Case	Rectum Volume (cc)	$D_{LEM 20\%}$ (38.7 Gy(RBE))	$D_{MKM 20\%}$ (28.8 Gy(RBE))	$D_{LEM 10\%}$ (54.7 Gy(RBE))	$D_{MKM 10\%}$ (46.4 Gy(RBE))	$D_{LEM 5\%}$ (65.1 Gy(RBE))	$D_{MKM 5\%}$ (60.0 Gy(RBE))	$D_{LEM 1\%}$ (69.3 Gy(RBE))	$D_{MKM 1\%}$ (66.0 Gy(RBE))
Prostate 1	68.6	26.3	14.0	50.9	38.1	61.4	50.7	67.1	63.3
Prostate 2	58.3	37.2	23.6	54.8	41.8	61.1	49.3	64.5	55.0
$L_{SAC}$ 1	146.2	47.2	35.1	59.9	50.8	63.8	56.3	67.9	62.7
$L_{SAC}$ 2	53.5	25.6	11.7	47.7	32.7	59.8	49.7	67.2	60.5
$H_{SAC}$ 1	86.0	48.6	37.0	58.8	49.4	63.3	54.8	67.7	60.5

Equivalent uniform doses (EUDs) and the corresponding NTCPs were calculated from each patient’s  $D_{MKM}$  distribution with FRoG, using G1 toxicity parameters reported by Fukahori et al., and are presented in Figure 4.

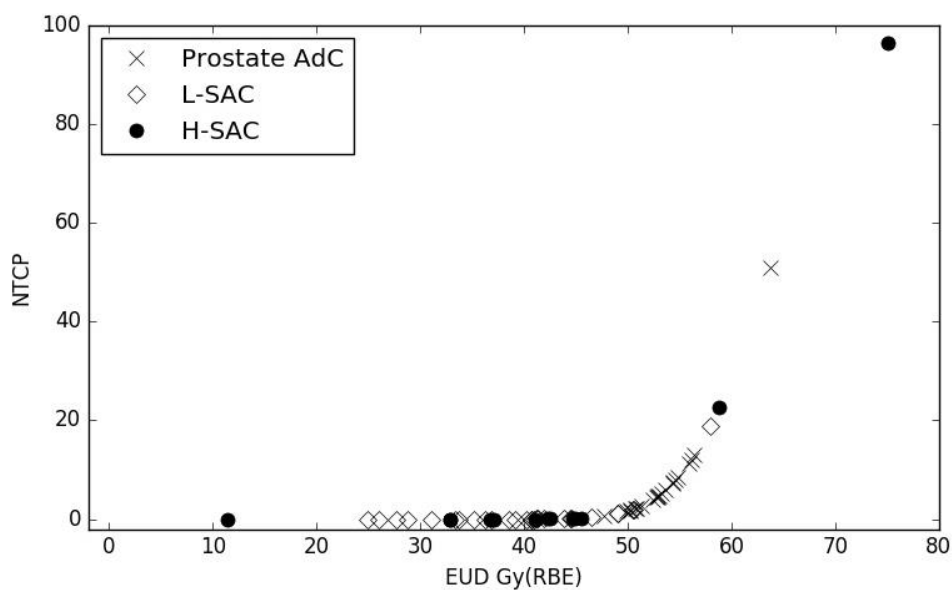


**Figure 4.** Late rectal toxicity normal tissue complication probability (NTCP) values as a function of rectum equivalent uniform doses (EUD) for prostate adenocarcinoma (AdC) (cross),  $L_{SAC}$  (empty diamonds) and  $H_{SAC}$  (full circles) patients.

The average EUDs were 53.3 Gy(RBE) (CI 95% 52.0–54.6), 38.2 Gy(RBE) (35.2–41.2) and 39.8 Gy(RBE) (31.9–47.7) for prostate,  $L_{SAC}$  and  $H_{SAC}$  groups, while the corresponding NTCP values were 5.23% (CI 95% 3.41–7.85), 0.00% (0.00–0.02), and 0.01% (0.00–0.62), respectively. Lower EUD and NTCP values reported for sacrum cases result from the stricter constraints applied during plan optimization. The resulting average value for the NTCP is in agreement with early clinical outcomes: over all the prostate AdC and sacral chordoma patients treated at CNAO, no rectal complication higher than G0 was reported at follow-up longer than 6 months. One patient from the  $H_{SAC}$  group showed a very high NTCP for late rectal toxicity (96.4%). This patient had a large planning target volume (3800 cc) compressing the rectum (144 cc) for the whole extent of the posterior rectal wall, widely involved in the high dose treatment area. However, it should be noted that the patient’s last follow-up was at

20 months, shorter than the minimum follow-up of patients included in the Japanese NTCP study (>36 months).

### 3. Discussion

Dose constraints for OARs in CIRT are not yet completely established. To take advantage of the long-term experience of NIRS, where patients have been treated with carbon ions since 1994 [20], we adopted the same fractionation schemes as NIRS for most clinical protocols, while modifying prescription doses to account for  $D_{RBE}$  dependence based on the RBE model [3,5]. In contrast, the optimization constraints for several OARs (e.g., optic structures, brainstem and rectum) were conservatively taken from Japanese clinical practice [21] without any correction. This approach could eventually compromise target coverage and result in a sub-optimal treatment. After 5 years of clinical experience based on evaluation of plan robustness, optimization of adaptive protocols and analysis of normal tissue toxicities, we could redefine LEM-based constraints for the optic pathways [15] and brainstem. In this work, we used the same approach to update and harmonize rectum constraints for all treatments based on a 16-fraction schedule.

Observed rectal toxicity among pelvic patients treated at CNAO was very low. According to the Common Terminology Criteria for Adverse Events version 4.03 (CTCAE) (U.S. Department of Health and Human Services, Washington, DC, USA) [22] scale, from the prostate AdC group, one case of rectal bleeding G1 was reported at three months of follow-up and resolved by the ninth month of follow-up. Concerning sacral chordoma patients, three cases of acute proctitis G1 were reported during treatment. Of these, one patient was lost at follow-up and the other two cases of gastrointestinal (GI) disorder were resolved at first follow-up. Concerning late complications, no bleeding nor signs of rectal wall damage were observed. As reported in the results section,  $D_{MKM}VHs$  lie largely below original MKM constraints, as demonstrated by the promising results for clinical outcome reported to date regarding rectal damage.

When comparing dose quantities calculated with a different treatment planning system (TPS), uncertainties must be taken into account affecting both absorbed and RBE-weighted dose distributions [5]. The expected differences between NIRS and CNAO dose computation systems are, in part, the rationale underlying the over-conservative, no-correction approach applied to OARs constraints at the beginning of clinical activity at CNAO. Both Syngo and FROG were validated against the Fluka-MC code [18,23] to guarantee dosimetric accuracy and, along with that, dosimetric agreement between the two systems. Finally, the translation of the  $D_{RBE|V}$  values was performed in the same calculation frame (using FROG) and was therefore not affected by the previously mentioned sources of dose deviation. Ultimately, the goal of deriving new constraints was to improve treatment quality in terms of tumor control, with a negligible increase in healthy tissue toxicity, and therefore, the implementation of these constraints to clinical practice must be performed with caution.

Also, uncertainties must be accounted for when applying NTCP parameters to a patient population different from the one they were optimized for [24]. For sacral chordoma patients, we applied an NTCP model based on prostate AdC patient toxicity outcomes, on the grounds that the rectum dose was delivered in the same number of fractions. Dose deviations between the two calculation systems from which the DVHs and EUD values were extracted could affect the NTCP results. In addition, the Japanese patient follow-ups were significantly longer (>36 months) than the follow-ups for our patient cohort. Taking these uncertainties into account, the estimated probability of late rectal complications was very low. In Okonogi et al.,  $D_{MKM|2cc}$  was found to be the most significant predictive factor for late rectal morbidities, with a threshold of 57.3 Gy(RBE) to limit the risk for a 20 fraction treatment schedule [17]. Under the hypothesis that schedules could be compared based on the biological effective dose (BED) concept, the corresponding 16 fraction threshold value, assuming an  $\alpha/\beta$  ratio of 3.9 Gy for the rectum [25], would be 53.5 Gy(RBE). Over our patient cohort, the average  $D_{MKM|2cc}$  was  $(34.7 \pm 11.1)$  Gy(RBE) with only one  $H_{SAC}$  patient exceeding the 16 fraction threshold ( $D_{MKM|2cc} = 55.8$  Gy(RBE)). This last case corresponds to the highest NTCP value described in the results section.

From NIRS NTCP analysis, the rectum appears as a serial organ regarding late complications, in agreement with conclusions from Okonogi et al. [17] Therefore, in the definition of updated constraints, focus was given to high rectum doses. The new values were expressed in cc to overcome the previously discussed differences determined by rectum size variation.

Based on the results presented in this work, for all future pelvic patient plan optimizations receiving a 16 fraction schedule, we set new rectum constraints to  $D_{1cc} \leq 66$  Gy(RBE) and  $D_{5cc} \leq 61$  Gy(RBE). A limit of  $D_{10cc} \leq 54$  Gy(RBE) will also be applied, without compromising target coverage. In Figure 5, new constraints are plotted together with the previously applied  $D_{MKM|v}$  and the translated  $D_{LEM|v}$ , where volume percentages have been translated to absolute values from the average rectal volume of the prostate AdC and sacral chordoma groups, respectively. The new  $D_{1cc}$  constraint will, on average, lie below the lower CI bound of translated  $D_{LEM|v}$  for both patient groups; while  $D_{5cc}$  has been established as the mean value of average extrapolated  $D_{LEM|v}$  for prostate and sacrum cases (also plotted in Figure 5), at the corresponding volume size of 5 cc. These constraints lie inside the range of protocol values defined at MedAustron (Wiener-Neustadt, Austria) for the CIRT of pelvic tumors, based on the same fractionation scheme in use at CNAO. Two particular sets of constraints are in clinical use: a lower dose level defined as optimal (MedAustron-O), and a higher dose level defined as acceptable (MedAustron-A). Uhl et al. reported HIT plan optimization constraints for patients with sacro-coccygeal chordoma, treated with a 16-fraction CIRT schedule [25]. The authors defined a structure corresponding to the overlap of the planning target volume and the rectum, to which a maximum dose constraint of 57.6 Gy(RBE) was assigned.

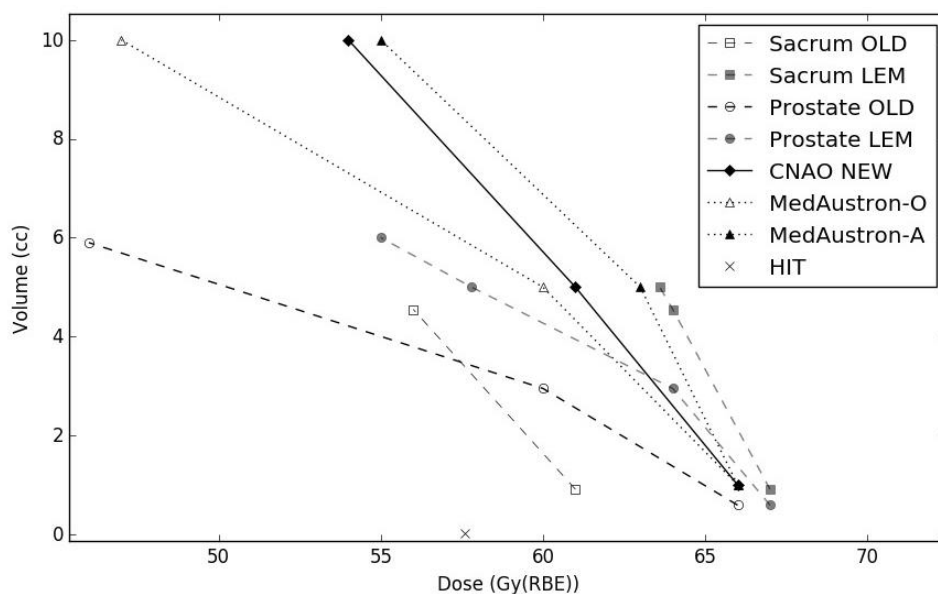


**Figure 5.** Rectum dose-volume constraints: old clinically applied values (Sacral chordoma—open square; prostate AdC—open circle), LEM-translated (Sacral chordoma—full square; prostate AdC full circle), new clinically defined (full diamond), MedAustron optimal (open triangle), MedAustron acceptable (full triangle), Heidelberg Ion-Beam Therapy Center (HIT) (cross).

## 4. Materials and Methods

### 4.1. Patient Treatment and Follow-Up

A total of 63 representative patients, treated for a tumor in the pelvis, were selected for this study: 22 prostate AdC cases, and 41 sacral chordoma cases. High-risk prostate AdC patients were consecutively treated between July 2013 and June 2017, with a dose prescription of 66.4 Gy(RBE) and results analyzed after a median follow-up time of 33 months (range: 14–62). In the analysis, 28 additional sacral chordoma cases treated with 70.4 Gy(RBE) ( $L_{SAC}$ ), and 13 additional cases treated with 73.6

Gy(RBE) ( $H_{SAC}$ ) between April 2013 and July 2018, were included, with a median follow up time of 39 months (range: 12–72) and 20 months (range: 8–70) for the  $L_{SAC}$  and  $H_{SAC}$  populations, respectively.

For treatment simulation and delivery, patients were positioned on a personalized cushion and immobilized with a solid thermoplastic mask, to optimize set-up reproducibility and minimize inter- and intra-fraction uncertainties. The patient set-up verification makes use of two orthogonal X-ray acquisitions for the registration of the bone anatomy, as well as a cone-beam CT (computed tomography)-scan for organ filling control. All patients received the CIRT in 16 fractions, 4 days-a-week, delivered with a pencil beam scanning technique. Prostate AdC patients were treated in a supine position, with two lateral-opposed fields, while sacral chordoma patients were treated in prone position with a minimum of three fields (two lateral-opposed and one vertical), unless for completely lateralized lesions. Periodic re-evaluation CT-scans were planned for every two weeks of treatment (8 fractions), except for in the case of patient-specific clinical indications.

The rectum volume was defined using the planning CT-scan, according to the Radiation Therapy Oncology Group (RTOG) contouring guidelines, starting inferiorly from the lowest level of the ischial tuberosity (right or left). Contouring ended superiorly before the rectum lost its round shape in the axial plane and connects anteriorly with the sigmoid [26].

All the rectum contours were independently reviewed by two medical doctors for compliance with guidelines.

The mean rectum volume was  $(80 \pm 36)$  cc over the whole patient population, with an average of  $(59 \pm 15)$  cc for prostate and  $(91 \pm 39)$  cc for sacrum cases. The average rectum volume size is affected by the different preparations patients undergo—according to the specific treatment protocol—and by clinical baseline conditions. The prostate AdC patients were routinely prepared with an enema before imaging and treatment, whereas no specific measure was employed for sacral chordoma patients. Moreover, rectum volumes were generally larger in the latter group due to tumor involvement with the sacral nerves causing the relaxation of the rectal wall.

Currently applied rectum dose constraints for a 16 fraction prostate AdC treatment are: dose to volume percentage  $v$ —5% and 1% ( $D_v$ ) lower than 60 and 66 Gy(RBE), respectively. In addition,  $D_v$  limits are set to minimize rectum lower doses to 20% and 10% of the volume, to 28.8 Gy(RBE) and 46.4 Gy(RBE), respectively, which can be compromised to prioritize target coverage. These  $D_v$  values fit a rectum upper boundary  $D_{MKM}VH$ , provided by NIRS colleagues, routinely taken as a reference for prostate AdC plan approval. In consideration of the larger rectum volumes involved, and considering the lower reproducibility in the rectum filling, shape and position of sacral chordoma patients, the  $D5\%$  and  $D1\%$  described values were applied to a planning risk volume, obtained with a uniform 5 mm expansion of the rectum. Rectum constraints were therefore slightly lower:  $D5\% \leq 56$  Gy(RBE) and  $D1\% \leq 61$  Gy(RBE). This approach was conceived with the aim of accounting for anatomical changes which could only be detected with the aid of periodic re-evaluation CT scans.  $D20\%$  and  $D10\%$  were not considered for the plan optimization of sacral chordoma cases.

Follow-up visits for the prostate AdC patients are scheduled at three, six and twelve months after treatment completion; every six months for the following two years and yearly afterwards, until the fifth year from the treatment. The patients will undergo a clinical examination, with a three-monthly evaluation of prostate-specific antigen and testosterone levels. A magnetic resonance imaging (MRI) scan and uroflowmetry will also be performed yearly.

Sacral chordoma patients will undergo follow-up visits, every three months for the first two years, and every six months for the following three years, with a clinical examination and an MRI scan. A thorax CT scan and whole spine MRI will be performed annually.

Gastrointestinal (GI) complications were scored according to the GI disorders terms of the CTCAE. In Fukahori et al. [16], GI complications were scored according to the guidelines of the Radiation therapy Oncology Group (RTOG) and the European Organization for Research and Treatment of Cancer (EORTC) [27]. With the aim of applying NIRS NTCP parameters to CNAO rectum DVHs, the toxicity originally reported according to CTCAE was re-scored for this analysis using the RTOG scale.

Patients analyzed in the paper cannot be identified as all the research has been conducted with anonymous data. All patients enrolled in the clinical trials gave their free informed consent to the treatment and the use of their data for research purposes. All the patients enrolled at CNAO freely signed their consent to the treatment and to the management of their clinical data, in an anonymized way, for research purposes.

Most of the clinical cases enquired were enrolled in clinical trials:

- CNAO S16/2012C Approved by referral Ethics Committee “CNAO” on 19 December 2012, “Phase II clinical trial on high risk prostate cancer treated by carbon ions radiation therapy”.
- CNAO S13/2012/C Approved on 21 December 2016, by referral Ethics Committee “Area Pavia”, “Phase II clinical trial on trunk sarcoma (of bones and of soft tissues) treated by carbon ions radiation therapy”.
- CNAO 33 2016 C “Sacral Chordoma: a Randomized & Observational study on surgery versus definitive radiation therapy in primary localized disease (SACRO)” approved on 24 November 2016, by referral Ethics Committee “Area Pavia”.

#### 4.2. Dose Recalculation and Analysis

All the treatment plans for the patient group treated in the pelvic region were calculated for clinical purposes with the Syngo PT (Siemens AG healthcare, Erlangen, Germany) TPS. CT image, RTdose, RTstructure and RTplan DICOM files were exported from Syngo and imported in FROG for the recalculation of  $D_{LEM}$  and  $D_{MKM}$ .

From the two corresponding rectum DVHs, patient-specific  $D_{MKM|v}$  values ( $v$ : 1%, 5%, 10%, 20%), were extracted and plotted as a function of the corresponding  $D_{LEM|v}$ . New  $D_{LEM|v}$  values translated from the original  $D_{MKM|v}$  constraints were determined from these plots. The regression was performed with Scipy libraries providing numerical integration, interpolation, optimization, linear algebra and statistics [28], and the software IBM SPSS Statistics for Windows, Version 26.0 (IBM Corp., Armonk, NY, USA). The average rectum DVHs over the patient population, in the two RBE systems, were evaluated in relation to original  $D_{MKM|v}$  and translated  $D_{LEM|v}$  constraints.

Five patients (2 prostate cases, 2  $L_{SAC}$  cases and 1  $H_{SAC}$  case) were randomly selected for optimized treatment plans with the new translated  $D_{LEM|v}$  constraints. The lower boundary values of the 95% CI were considered for  $D_{LEM|v}$  to account for uncertainties involved in the  $D_{RBE}$  translation process. Plan optimization was performed with Syngo and dose distributions were then exported to FROG for  $D_{MKM}$  recalculation. Rectum  $D_{MKM}$  DVHs were then analyzed to verify their compliance with the original  $D_{MKM|v}$  constraints.

From  $D_{MKM}$  distributions, the FROG generated EUD values to predict the late rectal toxicity NTCP, based upon the formulation reported by Fukahori et al. [16,29,30]. In particular, the median values for LKB parameters  $n$ ,  $m$  and TD50 (0.035 (95% CI: 0.024–0.047), 0.10 (0.084–0.13) and 63.6 Gy(RBE) (61.8–65.4)) obtained for  $\geq G1$  late rectal toxicity were selected to calculate the NTCP for the CNAO population.

A scheme summarizing the study methodology is presented in Figure 6, highlighting the two lines of investigation followed in this work. On one side, the conversion process of rectum dose distribution for 63 patients allowed the translation of  $D_{RBE}$  values between different RBE models. This part of the analysis provided a quantification of the potential for relaxation of LEM-based constraints. Concurrently, the follow-up of our pelvic patient cohort was analyzed to evaluate actual reported rectal toxicity. The recently published NTCP model from the Japanese NIRS group [16] was then applied to our dataset to estimate the probability of late rectal damage based on treatment outcomes registered with a longer follow-up. This second part of the study aimed at ensuring the absence of a significant toxicity rate with the currently applied constraints. New rectum dose constraints, to be confirmed prospectively using the clinical data, were finally defined for all the pelvic treatments scheduled in 16 fractions.

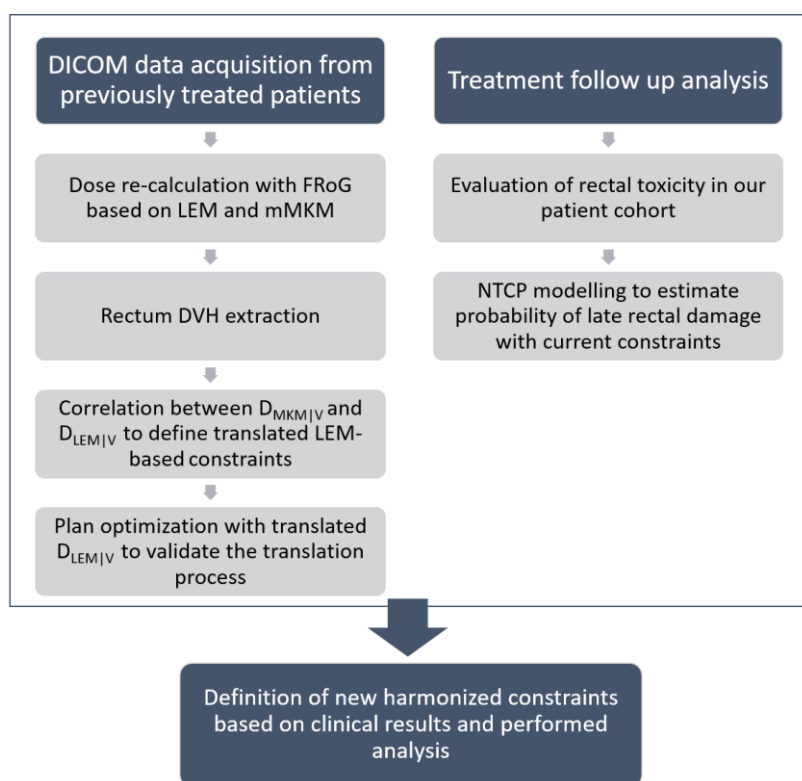


**Figure 6.** A scheme summarizing the study methodology.

## 5. Conclusions

For the definition of new OAR dose constraints, a detailed RBE model translation analysis has been combined with the evaluation of treatment toxicity, based on long-term clinical follow-up data and normal tissue complication predictors, as estimated by other reference CIRT centers. With the clinical implementation of updated dose constraints, we expect an improvement of treatment quality by allowing a potentially higher dose delivery to the tumor, with no increase in healthy tissue toxicity. The methodology applied in this work was successfully followed for the optic pathways [15] and brainstem. Updating dose constraints for organs at risk in the treatment of pancreatic AdC tumors and other abdominal lesions (i.e., duodenum, stomach, small bowel and colon) is currently ongoing.

**Author Contributions:** S.M. wrote the main manuscript text with K.C. as assistant author. K.C. was one of the developers, with A.M. (Andrea Mairani) as the lead designer of the project FRoG. K.C. performed all the data analysis under the supervision of A.M. (Andrea Mairani), S.M., S.R., and A.M. (Alfredo Mirandola) optimized the clinical treatment plans as Medical Physicists, with M.R.F., B.V. and P.F. as Medical Doctors. S.M. and S.R. collected the patient data. M.R.F. and B.V. were responsible for the treatment protocols and analyzed the patient follow-ups together with R.P., I.T. reviewed all the volume contours. J.E.D., S.M. and P.F. contributed to the definition of the study methodology. M.C. and F.V. provided clinical direction during the project's development. All authors have read and agreed to the published version of the manuscript.

**Funding:** This research received no external funding.

**Conflicts of Interest:** The authors declare no conflicts of interest.

## References

1. Kamada, T.; Tsujii, H.; Blakely, E.A.; Debus, J.; De Neve, W.; Durante, M.; Jäkel, O.; Mayer, R.; Orecchia, R.; Pötter, R.; et al. Carbon ion radiotherapy in Japan: An assessment of 20 years of clinical experience. *Lancet Oncol.* **2015**, *16*, e93–e100. [\[CrossRef\]](#)
2. Steinsträter, O.; Grün, R.; Scholz, U.; Friedrich, T.; Durante, M.; Scholz, M. Mapping of RBE-weighted doses between HIMAC- and LEM-based treatment planning systems for carbon ion therapy. *Int. J. Radiat. Oncol. Biol. Phys.* **2012**, *84*, 854–860. [\[CrossRef\]](#)

3. Fossati, P.; Molinelli, S.; Matsufuji, N.; Ciocca, M.; Mirandola, A.; Mairani, A.; Mizoe, J.; Hasegawa, A.; Imai, R.; Kamada, T.; et al. Dose prescription in carbon ion radiotherapy: A planning study to compare NIRS and LEM approaches with a clinically-oriented strategy. *Phys. Med. Biol.* **2012**, *57*, 7543–7554. [[CrossRef](#)]
4. Fossati, P.; Matsufuji, N.; Kamada, T.; Karger, C.P. Radiobiological issues in prospective carbon ion therapy trials. *Med. Phys.* **2018**, *45*, e1096–e1110. [[CrossRef](#)]
5. Molinelli, S.; Magro, G.; Mairani, A.; Matsufuji, N.; Kanematsu, N.; Inaniwa, T.; Mirandola, A.; Russo, S.; Mastella, E.; Hasegawa, A.; et al. Dose prescription in carbon ion radiotherapy: How to compare two different RBE-weighted dose calculation systems. *Radiother. Oncol.* **2016**, *120*, 307–312. [[CrossRef](#)]
6. Scholz, M.; Kellerer, A.M.; Kraft-Weyrather, W.; Kraft, G. Computation of cell survival in heavy ion beams for therapy. *Radiat. Environ. Biophys.* **1997**, *36*, 59–66. [[CrossRef](#)] [[PubMed](#)]
7. Kramer, M.; Scholz, M. Treatment planning for heavy-ion radiotherapy: Calculation and optimization of biologically effective dose. *Phys. Med. Biol.* **2000**, *45*, 3319–3330. [[CrossRef](#)] [[PubMed](#)]
8. Kanai, T.; Endo, M.; Minohara, S.; Miyahara, N.; Koyama-ito, H.; Tomura, H.; Matsufuji, N.; Futami, Y.; Fukumura, A.; Hiraoka, T.; et al. Biophysical characteristics of HIMAC clinical irradiation system for heavy-ion radiation therapy. *Int. J. Radiat. Oncol. Biol. Phys.* **1999**, *44*, 201–210. [[CrossRef](#)]
9. Inaniwa, T.; Furukawa, T.; Kase, Y.; Matsufuji, N.; Toshito, T.; Matsumoto, Y.; Furusawa, Y.; Noda, K. Treatment planning for a scanned carbon beam with a modified microdosimetric kinetic model. *Phys. Med. Biol.* **2010**, *55*, 6721–6737. [[CrossRef](#)]
10. Inaniwa, T.; Kanematsu, N.; Matsufuji, N.; Kanai, T.; Shirai, T.; Noda, K.; Tsuji, H.; Kamada, T.; Tsujii, H. Reformulation of a clinical-dose system for carbon-ion radiotherapy treatment planning at the National Institute of Radiological Sciences, Japan. *Phys. Med. Biol.* **2015**, *60*, 3271–3286. [[CrossRef](#)]
11. Michalski, J.M.; Gay, H.; Jackson, A.; Tucker, S.L.; Deasy, J.O. Radiation Dose-Volume Effects in Radiation-Induced Rectal Injury. *Int. J. Radiat. Oncol. Biol. Phys.* **2010**, *76*, S123–S129. [[CrossRef](#)] [[PubMed](#)]
12. Katoh, H.; Tsuji, H.; Ishikawa, H.; Kamada, T.; Wakatsuki, M.; Hirasawa, N.; Suzuki, H.; Akakura, K.; Nakano, T.; Shimazaki, J.; et al. Health-related quality of life after carbon-ion radiotherapy for prostate cancer: A 3-year prospective study. *Int. J. Urol.* **2014**, *21*, 370–375. [[CrossRef](#)] [[PubMed](#)]
13. Schaake, W.; van der Schaaf, A.; van Dijk, L.V.; Bongaerts, A.H.; van den Bergh, A.C.; Langendijk, J.A. Normal tissue complication probability (NTCP) models for late rectal bleeding, stool frequency and fecal incontinence after radiotherapy in prostate cancer patients. *Radiother. Oncol.* **2016**, *119*, 381–387. [[CrossRef](#)] [[PubMed](#)]
14. Magro, G.; Dahle, T.J.; Molinelli, S.; Ciocca, M.; Fossati, P.; Ferrari, A.; Inaniwa, T.; Matsufuji, N.; Ytre-Hauge, K.S.; Mairani, A. The FLUKA Monte Carlo code coupled with the NIRS approach for clinical dose calculations in carbon ion therapy. *Phys. Med. Biol.* **2017**, *62*, 3814–3827. [[CrossRef](#)] [[PubMed](#)]
15. Dale, J.E.; Molinelli, S.; Vitolo, V.; Vischioni, B.; Bonora, M.; Magro, G.; Pettersen, H.E.S.; Mairani, A.; Hasegawa, A.; Dahl, O.; et al. Optic nerve constraints for carbon ion RT at CNAO-reporting and relating outcome to European and Japanese RBE. *Radiother. Oncol.* **2019**, *140*, 175–181. [[CrossRef](#)] [[PubMed](#)]
16. Fukahori, M.; Matsufuji, N.; Himukai, T.; Kanematsu, N.; Mizuno, H.; Fukumura, A.; Tsuji, H.; Kamada, T. Estimation of late rectal normal tissue complication probability parameters in carbon ion therapy for prostate cancer. *Radiother. Oncol.* **2016**, *118*, 136–140. [[CrossRef](#)] [[PubMed](#)]
17. Okonogi, N.; Fukahori, M.; Wakatsuki, M.; Ohkubo, Y.; Kato, S.; Miyasaka, Y.; Tsuji, H.; Nakano, T.; Kamada, T. Dose constraints in the rectum and bladder following carbon-ion radiotherapy for uterus carcinoma: A retrospective pooled analysis. *Radiat. Oncol.* **2018**, *13*, 119. [[CrossRef](#)]
18. Choi, K.; Mein, S.B.; Kopp, B.; Magro, G.; Molinelli, S.; Ciocca, M.; Mairani, A. FRoG—A new calculation engine for clinical investigations with proton and carbon ion beams at CNAO. *Cancers* **2018**, *10*, 395. [[CrossRef](#)]
19. Mein, S.; Choi, K.; Kopp, B.; Tessonnier, T.; Bauer, J.; Ferrari, A.; Haberer, T.; Debus, J.; Abdollahi, A.; Mairani, A. Fast robust dose calculation on GPU for high-precision  $^1\text{H}$ ,  $^4\text{He}$ ,  $^{12}\text{C}$  and  $^{16}\text{O}$  ion therapy: The FRoG platform. *Sci. Rep.* **2018**, *8*, 14829. [[CrossRef](#)]
20. Tsujii, H.; Mizoe, J.E.; Kamada, T.; Baba, M.; Kato, S.; Kato, H.; Tsuji, H.; Yamada, S.; Yasuda, S.; Ohno, T.; et al. Overview of clinical experiences on carbon ion radiotherapy at NIRS. *Radiother. Oncol.* **2004**, *73*, S41–S49. [[CrossRef](#)]

21. Hasegawa, A.; Mizoe, J.; Jingu, K.; Bessho, H.; Morikawa, T.; Kamada, T.; Tsujii, H. Carbon Ion Radiotherapy for Malignant Head-and-Neck Tumors Invading the Skull Base. *Int. J. Radiat. Oncol. Biol. Phys.* **2010**, *78*, 173. [[CrossRef](#)]
22. NCI National Cancer Institute (US). *Common Terminology Criteria for Adverse Events (CTCAE) Version 4.03*; NIH Publication: Bethesda, MD, USA, 2010.
23. Bauer, J.; Sommerer, F.; Mairani, A.; Unholtz, D.; Farook, R.; Handrack, J.; Frey, K.; Marcelos, T.; Tessonnier, T.; Ecker, S.; et al. Integration and evaluation of automated Monte Carlo simulations in the clinical practice of scanned proton and carbon ion beam therapy. *Phys. Med. Biol.* **2014**, *59*, 4635–4659. [[CrossRef](#)] [[PubMed](#)]
24. Marks, L.B.; Yorke, E.D.; Jackson, A.; Ten Haken, R.K.; Constine, L.S.; Eisbruch, A.; Bentzen, S.M.; Nam, J.; Deasy, J.O. Use of normal tissue complication probability models in the clinic. *Int. J. Radiat. Oncol. Biol. Phys.* **2010**, *76*, S10–S19. [[CrossRef](#)] [[PubMed](#)]
25. Uhl, M.; Edler, L.; Jensen, A.D.; Habl, G.; Oelmann, J.; Röder, F.; Jäckel, O.; Debus, J.; Herfarth, K. Randomized phase II trial of hypofractionated proton versus carbon ion radiation therapy in patients with sacrococcygeal chordoma—the ISAC trial protocol. *Radiat. Oncol.* **2014**, *9*, 100. [[CrossRef](#)] [[PubMed](#)]
26. Gay, H.A.; Barthold, H.J.; O’Meara, E.; Bosch, W.R.; El Naqa, I.; Al-Lozi, R.; Rosenthal, S.A.; Lawton, C.; Lee, W.R.; Sandler, H.; et al. Pelvic normal tissue contouring guidelines for radiation therapy: A radiation therapy oncology group consensus panel atlas. *Int. J. Radiat. Oncol. Biol. Phys.* **2012**, *83*, e353–e562. [[CrossRef](#)] [[PubMed](#)]
27. Cox, J.D.; Stetz, J.; Pajak, T.F. Toxicity criteria of the Radiation Therapy Oncology Group (RTOG) and the European Organization for Research and Treatment of Cancer (EORTC). *Int. J. Radiat. Oncol. Biol. Phys.* **1995**, *31*, 1341–1346. [[CrossRef](#)]
28. Scipy.org. Available online: <http://www.scipy.org/> (accessed on 16 September 2019).
29. Lyman, J.T. Complication Probability as Assessed from Dose-Volume Histograms. *Radiat. Res. Suppl.* **1985**, *8*, S13–S19. [[CrossRef](#)]
30. Burman, C.; Kutcher, G.J.; Emami, B.; Goitein, M. Fitting of normal tissue tolerance data to an analytic function. *Int. J. Radiat. Oncol. Biol. Phys.* **1991**, *21*, 123–135. [[CrossRef](#)]



© 2019 by the authors. Licensee MDPI, Basel, Switzerland. This article is an open access article distributed under the terms and conditions of the Creative Commons Attribution (CC BY) license (<http://creativecommons.org/licenses/by/4.0/>).